Atmospheric Sciences Letters
doi:10.1006/asle.2000.0002

A Linear Diagnosis of the Coupled Extratropical Ocean–Atmosphere System in the GFDL GCM

Matthew Newman, Michael A. Alexander, Christopher R. Winkler, James D. Scott and Joseph J. Barsugli

NOAA-CIRES Climate Diagnostics Center, University of Colorado, Boulder, CO 80309, U.S.A.

Summary: Diagnosing a coupled system with linear inverse modelling (LIM) can provide insight into the nature and strength of the coupling. This technique is applied to the cold season output of the GFDL GCM, forced by observed tropical Pacific SSTs and including a slab mixed layer ocean model elsewhere. It is found that extratropical SST anomalies act to enhance atmospheric thermal variability and diminish barotropic variability over the east Pacific in these GCM runs, in agreement with other theoretical and modelling studies. North-west Atlantic barotropic variability is also enhanced. However, all these feedbacks are very weak. LIM results also suggest that North Pacific extratropical SST anomalies in this model would rapidly decay without atmospheric forcing induced by tropical SST anomalies.

1. INTRODUCTION

Understanding the nature and strength of atmosphere–ocean coupling in the extratropics is important on a variety of time scales. Recently Barsugli and Battisti (1998) suggested that the primary effect of coupling is to reduce the effective thermal damping of both sea surface temperature (SST) and surface air temperature; that is, it acts to enhance thermal variability.

Numerous GCM studies (e.g. Palmer and Sun, 1985; Pitcher *et al*., 1988; Ferranti *et al*., 1994; Peng *et al*., 1995; Peng and Whitaker, 1999) have used prescribed extratropical SST anomalies to force an atmospheric response. The nature of this response varies significantly from model to model, however, and is dependent upon details of the model including its climate. These studies, moreover, all suffer from the same drawback: the real system is *coupled*. An SST anomaly may be due to a pre-existing atmospheric anomaly and the SST anomaly may evolve in response to any atmospheric anomaly it

Corresponding author address: Dr Matthew Newman, NOAA-CIRES Climate Diagnostics Center, University of Colorado, Campus Box 449, Boulder, CO 80309-0449, U.S.A.; E-mail: men@cdc.noaa.gov

1530–261X

creates. Thus, fixed extratropical SST anomaly experiments can lead to incomplete ideas abut the nature of the real coupling.

Ideally, we would like to diagnose extratropical ocean–atmosphere coupling from observations, or from output of realistic coupled GCM simulations. Such diagnosis is often done using statistical methods based solely on simultaneous covariability relations between oceanic and atmospheric variables. But such an analysis cannot yield the normal modes and optimal growth structures of the coupled system, and cannot produce explicit knowledge of the feedback terms. (See Newman and Sardeshmukh, 1995 and Frankignoul *et al.* (1998) for further discussion of the drawbacks of simultaneous covariability statistics.)*

In this paper, we suggest that linear inverse modelling (LIM; e.g. Penland and Sardeshmukh, 1995; Penland, 1996; Branstator and Haupt, 1998; DelSole and Hou, 1999) is an effective technique to diagnose a coupled system *quantitatively*. As our example, we apply LIM to cold season output of a seasonally varying GCM, forced by observed tropical Pacific SSTs and including a slab mixed layer elsewhere. We must first ask: can this GCM dataset be usefully diagnosed with LIM; that is, can it be described in terms of linear dynamics driven by Gaussian white noise? If so, then we can proceed to ask: what are the impacts of extratropical air-sea coupling in the model?

2. LINEAR INVERSE MODELLING

Consider the general coupled system:

$$\frac{d\mathbf{x}_A}{dt} = \mathbf{F}_{AA}\mathbf{x}_A + \mathbf{F}_{OA}\mathbf{y}_O + \mathbf{R}_x$$
$$\frac{d\mathbf{y}_O}{dt} = \mathbf{F}_{OA}\mathbf{x}_A + \mathbf{F}_{OO}\mathbf{y}_O + \mathbf{R}_y \tag{1}$$

where $\mathbf{x}_A$ represents one or more atmospheric (A) state variables and $\mathbf{y}_O$ one or more oceanic (O) state variables. $\mathbf{F}_{ij}$ are the linear dependencies of variable j on variable i; $\mathbf{R}_x$ and $\mathbf{R}_y$ can represent non-linear terms and/or functions of state variables not contained in either $\mathbf{x}_A$ or $\mathbf{y}_O$.

We try to model (1) as:

$$\frac{d\mathbf{X}}{dt} = \mathbf{B}\mathbf{X} + \boldsymbol{\xi} \tag{2}$$

*Canonical Correlation Analysis (CCA) and Singular Value Decomposition (SVD) are two such methods. Note that even when these methods are applied to lagged data, they still fail in the manner described above.

where

$$\mathbf{B}=\begin{bmatrix}\mathbf{F}_{AA}\mathbf{F}_{OA}\\ \mathbf{F}_{AO}\mathbf{F}_{OO}\end{bmatrix},\quad \mathbf{X}=\begin{bmatrix}\mathbf{x}_A\\ \mathbf{y}_O\end{bmatrix} \tag{3}$$

and ξ is Gaussian noise which is white in time but can have finite spatial correlation. Equation (2) can be an excellent approximation to the fully non-linear system if the decorrelation time scale of the non-linearities in $\mathbf{R}_x$ and $\mathbf{R}_y$, is much shorter than the time scales of linear dynamics inherent to $\mathbf{B}$ (e.g. Hasselmann, 1976; Penland, 1996). Then linear analysis is appropriate to diagnose this coupled system.

The solution to eqn (2) is:

$$\mathbf{X}(t+\boldsymbol{\tau}_0)=\exp(\mathbf{B}\tau_0)\mathbf{X}(t)+\boldsymbol{\sigma}(t+\tau_0) \tag{4}$$

where $\boldsymbol{\sigma}(t+\tau_0)$ is a function of the stochastic forcing ξ integrated over the time interval $[t,t+\tau_0]$. From the theory of linear inverse modelling (LIM) (e.g. Penland and Sardeshmukh, 1995), eqn (4) is solved as:

$$\mathbf{B}=\frac{1}{\tau_0}\ln[\langle\mathbf{X}(t+\tau_0)\mathbf{X}(t)^T\rangle\langle\mathbf{X}(t)\mathbf{X}(t)^T\rangle^{-1}] \tag{5}$$

where T represents the matrix transpose, and brackets $\langle\ \rangle$ a time mean. Thus $\mathbf{B}$ (and hence, the feedback submatrices $\mathbf{F}_{ij}$) is estimated from the zero- and τ_0-lag covariance statistics of $\mathbf{X}$. Note that principal oscillation patterns (POPs; Hasselmann, 1988) are the normal modes of the (stable) $\mathbf{B}$ operator.

One important advantage of LIM over other linear statistical techniques is that its inherent assumptions, especially of linearity, are thoroughly testable. If eqn (2) is a good approximation of eqn (1), then the computation of $\mathbf{B}$ from eqn (5) should be roughly independent of lag τ_0. Also, since the forcing ξ has a Gaussian distribution, $\mathbf{X}$ should as well. Of course, if eqn (2) is a good model, it should produce good forecasts of $\mathbf{X}(t)$ given only $\mathbf{X}(0)$. Actual forecast error should evolve in a manner consistent with the derivation of the expected error $\boldsymbol{\sigma}(t+\tau)$, which can be determined from eqn (2) using standard methods of stochastic differential equations. A complete discussion of these and other tests of LIM can be found in Penland and Sardeshmukh (1995).

One drawback of many statistical models including LIM is the possibility that $\mathbf{R}_x$ and $\mathbf{R}_y$ linearly depend upon another variable (say, $\mathbf{v}$) which is not included in the specification of $\mathbf{x}_A$ and $\mathbf{y}_O$. In this case, LIM remains valid as long as $\mathbf{v}$ is a linear function of $\mathbf{x}_A$ and $\mathbf{y}_O$. Of course, it may not be clear

which variables are dependent and which are independent, which could obscure some questions of causation (Frankignoul, 1999).

3. MODEL DATA

We have applied LIM to output from the GFDL R30S14 "TOGA-ML" model runs (Alexander and Scott, 1995). The GCM varies seasonally, is forced by observed tropical Pacific SSTs, and has a 50-m slab mixed layer elsewhere over the global ocean. The model was run as a four-member ensemble for the years 1950–1995. Note that these runs are not entirely independent, since each member of the ensemble has the same tropical SST.

For the present analysis, the oceanic variable $\mathbf{y}_O$ is defined as a vector containing SST anomalies north of 20°S. The atmospheric variable $\mathbf{x}_A$ is defined as a vector containing 200 mb geopotential height anomalies and 850 mb geopotential height anomalies, also north of 20°S. Data are interpolated to a $5° \times 5°$ grid and averaged into monthly means for the November–March (NDJFM) period. Anomalies are determined as departures of the monthly mean from the corresponding climatological monthly mean, where the climatology is defined as both a time and ensemble mean.

Even with 180 winters of model output, there are not enough data to determine **B** accurately at every grid point. Also, we wish to avoid merely fitting data with as many numbers as there are degrees of freedom. Thus, we truncated the data in EOF space to the leading 30 geopotential height EOFs and the leading 20 SST EOFs. This truncation retains about 70% of domain-integrated variance for each field. Retaining either fewer or more EOFs produced a slightly poorer model, as measured by forecast skill.

4. RESULTS

To test the appropriateness of LIM in this case, we first see if it can outperform a lag-1 autoregression (AR-1) model. This is done by making forecasts of independent data with the LIM via a jack-knifing procedure: all four ensemble members of a given year were removed from the dataset, **B** was computed for $\tau_0 = 1$ month, and then that **B** was used to make both one- and two-month forecasts for the ensemble members of the missing year. Local anomaly correlations of jack-knifed LIM forecasts were compared with forecasts produced from a AR-1 model of 200 mb geopotential height. This was done by correlating time series of forecast anomalies with *untruncated* GCM anomalies at each grid point. Figure 1 shows that LIM forecasts are everywhere much better than AR-1 forecasts. Error variances (not shown) of the LIM forecasts are similarly improved.

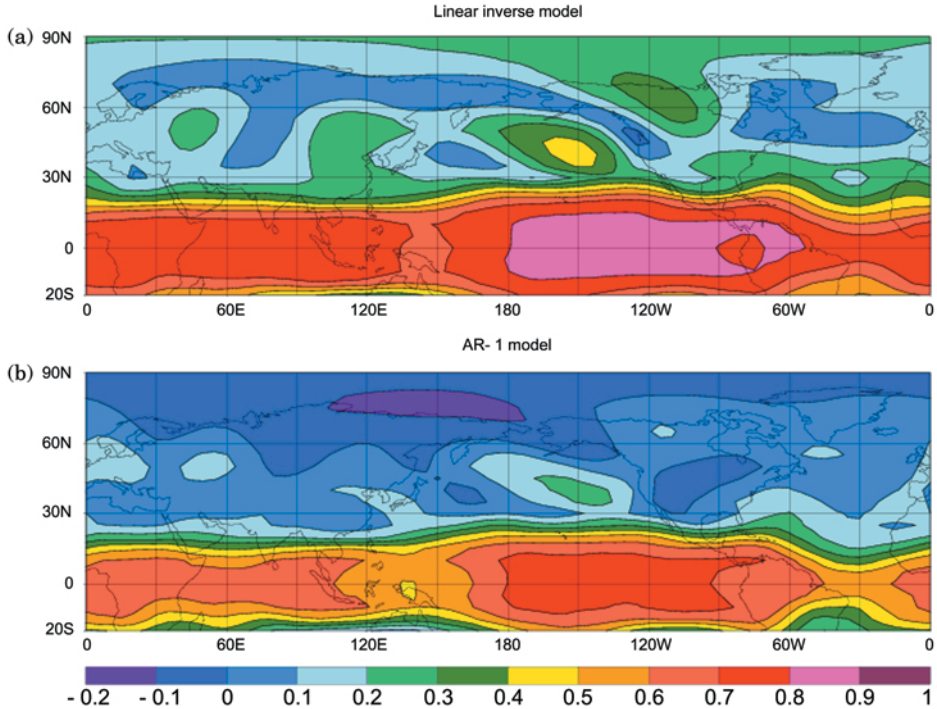

Figure 1. Local anomaly correlation of 200 mb geopotential height forecasts using a two-month forecast lead, for the four-member ensemble for NDJFM 1950/51–1994/95. (a) From the linear inverse model. (b) From the local AR-1 model. Contour interval is 0.1.

As a test of the effects of sampling, **B** was also computed from datasets from which one entire ensemble was removed. All results shown below were found to be qualitatively unchanged, although eigenvalues of eqn (6) did vary by up to 20%.

Other test results are similarly successful. For example, the distributions of all height and SST PCs cannot be distinguished from Gaussian distributions (as determined by a Kolmogorov–Smirnov test (e.g. Sardeshmukh *et al*., 2000) at the 95% significance level). Domain integrated error variance develops with forecast time in a manner consistent with theory (Penland and Sardeshmukh, 1995).

The inclusion of SST as a forecast variable improves the LIM forecast compared to an LIM which is derived from geopotential height alone.

Our final test also produces an interesting result concerning optimal growth structures. We have computed the eigenanalysis of:

$$\mathbf{G}(\tau)^T\mathbf{D}\mathbf{G}(\tau) \text{ and } \mathbf{G}(\tau)\mathbf{D}\mathbf{G}(\tau)^T \tag{6a,b}$$

where $\mathbf{G}=\exp(\mathbf{B}\tau)$ and $\mathbf{D}$ represents an L2 norm (that is, square integrable) of geopotential height only. It can be shown (e.g. Farrell, 1988; Penland and Sardeshmukh, 1995) that the initial condition which produces maximum global amplification of geopotential height anomalies will be the leading eigenvector of eqn (6a), which will evolve after a time period τ into the leading eigenvector of eqn (6b).

Figure 2 shows these leading eigenvectors. On the left is the initial condition which optimizes growth of Northern Hemisphere geopotential height anomalies. Two months later this pattern evolves into the pattern on the right. Thus, optimal growth is associated with an ENSO-like SST anomaly, which produces a strong extratropical anomalous height response reminiscent of the TNH pattern (Barnston and Livezey, 1987). At the same time, an SST anomaly of opposite sign to the tropical anomaly is induced in the central North Pacific. This feature is consistent with the atmospheric bridge (Alexander, 1992; Lau and Nath, 1996).

A strong test of LIM is whether growth structures determined by $\mathbf{G}(\tau)$ are really relevant to the development of anomalies in the full GCM. Figure 3 displays a scatterplot of the projection of GCM anomalies upon the leading optimal structure against the projection two months later of GCM geopotential height anomalies upon the leading growth structure. The high correlation between the two ordinates indicates the success of the LIM.

Since $\mathbf{B}$ does indeed represent relevant linear dynamics of the coupled system, we can investigate the feedbacks within it. Figure 4 displays the diagonal elements of the feedback submatrix $\mathbf{F}_{\mathrm{OA}}$, separated into SST feedbacks upon the baroclinic (that is, vertical difference) and barotropic (that is, vertical sum) portions of the two geopotential height levels after a month. As expected, SST acts locally to strongly enhance atmospheric thermal variability in the tropics. Extratropical thermal variability is also locally enhanced, in agreement with Barsugli and Battisti (1998). Interestingly, feedbacks enhance the barotropic atmospheric anomaly in the north Atlantic but *weaken* it in the central Pacific. This is consistent with results from an earlier version of this GCM, where it was found that the fixed slab mixed layer acted to slightly reduce upper-level atmospheric variability in the east Pacific (Bladé, 1999).

Localization of these feedbacks is a consequence of local characteristics of the time–mean height and SST fields. Nevertheless, we expect that the feedbacks are likely to be much more complex than

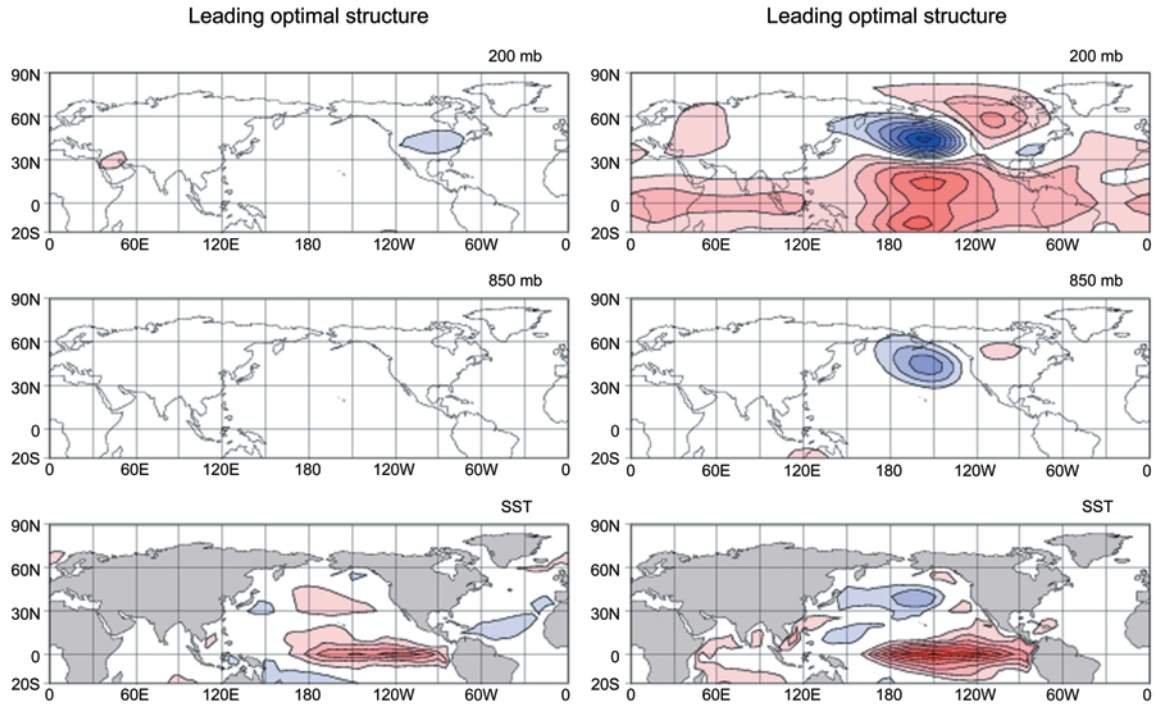

Figure 2. Left: Initial condition that maximizes the growth of geopotential height anomalies after two months. Right: Anomaly pattern two months after the initial condition shown in the left column. Contour interval is 0.1 K for SST anomalies and 5 m for height anomalies.

this simple picture, since we have not yet examined the offdiagonal elements of $\mathbf{F}_{OA}$. A full analysis would compute preferred *modes* of the feedback, which can be obtained from eigenvector analysis. This has not yet been done but is a straightforward calculation given **B**.

We also estimate the importance of the feedbacks by making forecasts with **B** and then repeating these forecasts with an altered **B** operator in which feedback of the extratropical SST upon the atmosphere is removed. Forecast anomalies for each set (not shown) are very similar. The feedback reduces geopotential height anomalies by less than 5% over the Pacific and increases anomalies by less

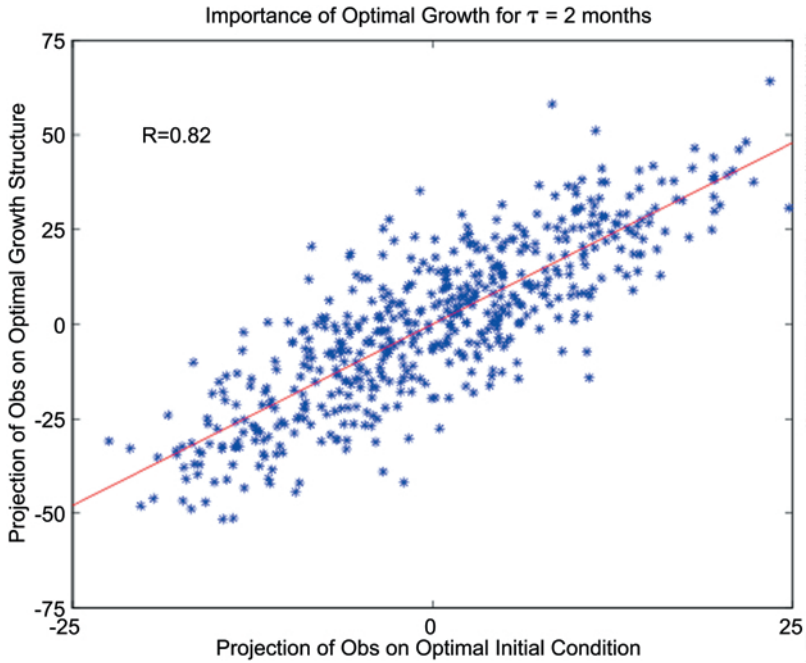

Figure 3. Projection of anomaly upon optimal growth structure vs projection of height anomaly on evolved structure two months later.

than 10% over the north Atlantic. This suggests that the extratropical SST effect upon the atmosphere is quite weak in these GCM simulations.

Finally, as a counterpoint to GCM experiments using fixed SST anomalies (discussed in the introduction), we can perform initial value experiments using eqn (2) as a surrogate for the full coupled GCM. We can thus see whether an atmospheric response will act to reinforce or reduce an initial SST anomaly. Two different cases are displayed in the two columns of Figure 5. In both cases, there is an initial midlatitude SST anomaly, but in case 1 (left panels) there is also an initial tropical SST anomaly of opposite sign. Both cases have no initial height anomaly. Note that since our system is linear, the response to a tropical SST anomaly alone can be obtained by subtracting the right panels from the left panels.

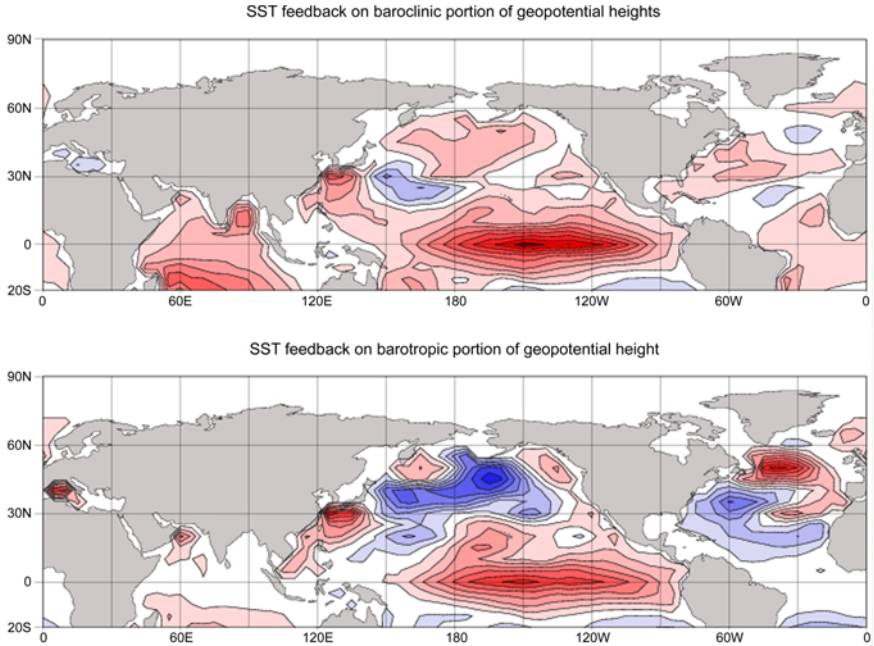

Figure 4. Local SST-atmosphere feedback coefficients. Red shading represents positive values; blue shading represents negative values. The zero contour has been omitted for clarity.

After one month, the tropical SST anomaly produces a strong atmospheric response which is only slightly stronger after another month. The SST anomaly weakens slowly, and persists for many months (not shown). But when there is an initial SST anomaly only in the extratropics, results are very different: a weak atmospheric response results one month later (not shown), but now the extratropical SST is reduced by about a third each month. Taken together, these experiments suggest that the decorrelation time scale of extratropical SST anomalies in the GCM is lengthened by a few months by coupling to an atmosphere which is in turn forced by tropical SST anomalies. Whether this is true in the real system (which has much more complex ocean dynamics than the simple fixed-depth mixed layer used here) remains to be determined. Nevertheless, these results suggest that in this model, a fixed extratropical SST anomaly would produce an unrealistic atmospheric response.

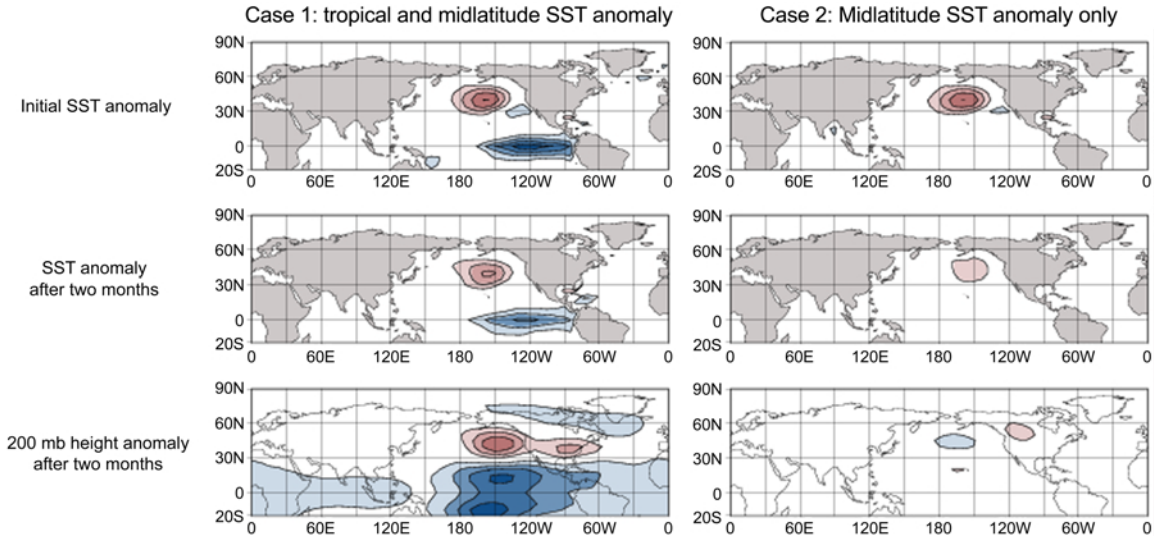

Figure 5. Linear response to an initial SST anomaly located in (left column) the tropics and midlatitudes or (right column) the midlatitudes only. Contour interval is 0.3 K for SST and 8 m for 200 mb heights.

5. SUMMARY

For these time scales, in this model, and at this time of year, linear inverse modelling has demonstrated that:

(1) The dominant growing Northern Hemisphere anomaly starts as an SST perturbation in the tropical Pacific, and develops into a TNH-like atmospheric pattern one month later.
(2) In the Pacific, extratropical SST anomalies may not be well maintained without atmospheric forcing, such as that induced by tropical SST anomalies (the atmospheric bridge).
(3) Linear feedback of extratropical SST upon geopotential height anomalies is weak.

We plan to use this technique on model runs with more sophisticated ocean models, and compare the feedbacks across the models. The same approach will also be applied to long integrations of other coupled GCMs. A more detailed examination of the feedback operators (that is, submatrices within **B**) is also currently underway.

Finally, we have had considerable success using LIM to model observed streamfunction and tropical heating from a 30-year data set (Winkler *et al.*, 1999). It may be possible to similarly determine **B** from observed atmosphere/SST fields, which we plan to attempt in the future.

Acknowledgements

It is a pleasure to thank Cécile Penland, Prashant Sardeshmukh, and Shileng Peng for stimulating and helpful discussions. This paper was improved by the comments of two anonymous reviewers.

References

Alexander, M. A., 1992. Midlatitude atmosphere–ocean interaction during El Nino. Part I: The North Pacific Ocean. *J. Clim.*, **5,** 944–958.

Alexander, M. A. and Scott, J. D., 1995. Atlas of climatology and variability in the GFDL R30S14 GCM. [Available at http://www.cdc.noaa.gov/~jds/atlas.html.]

Barnston, A. G. and Livezey, R., 1987. Classification, seasonality and persistence of low-frequency atmospheric circulation patterns. *Mon. Wea. Rev.*, **115,** 1083–1126.

Barsugli, J. J. and Battisti, D. S., 1998. The basic effects of atmosphere-ocean thermal coupling on midlatitude variability. *J. Atmos. Sci.*, **55,** 477–493.

Bladé, I., 1999. The influence of midlatitude ocean-atmosphere coupling on the low-frequency variability of a GCM. Part II: Interannual variability induced by tropical SST forcing. *J. Climate*, **12,** 21–45.

Branstator, G. and Haupt, S. E., 1998. An empirical model of barotropic atmospheric dynamics and its response to tropical forcing. *J. Climate*, **11,** 2645–2667.

DelSole, T. and Hou, A. Y., 1999. Empirical stochastic models for the dominant climate statistics of a General Circulation Model. *J. Atmos. Sci.*, **56,** 3436–3456.

Farrell, B., 1988. Optimal excitation of neutral Rossby waves. *J. Atmos. Sci.*, **45,** 163–172.

Ferranti, L., Molteni, F. and Palmer, T. N., 1994. Impact of localized tropical and extratropical SST anomalies in ensembles of seasonal GCM integrations. *Quart. J. Roy. Met. Soc.*, **120,** 1613–1645.

Frankignoul, C., Czaja, A. and L'Heveder, B., 1998. Air-sea feedback in the North Atlantic and surface boundary conditions for ocean models. *J. Clim.*, **11,** 2310–2324.

Frankignoul, C., 1999. A cautionary note on the use of statistical atmospheric models in the middle latitudes: Comments on "Decadal variability in the North Pacific as simulated by a hybrid coupled model". *J. Climate*, **12,** 1871–1872.

Hasselmann, K., 1976. Stochastic climate models. Part I: Theory. *Tellus*, **28,** 474–485.

Hasselmann, K., 1988. PIPs and POPs—A general formalism for the reduction of dynamical systems in terms of Principal Interaction Patterns and Principal Oscillation Patterns. *J. Geophys. Res.*, **93,** 11 105–11 021.

Lau, N.-C. and Nath, M. J., 1996. The role of the "atmospheric bridge" in linking tropical Pacific ENSO events to extratropical SST anomalies. *J. Clim.*, **9,** 2036–2057.

Newman, M. and Sardeshmukh, P. D., 1995. A caveat concerning singular value decomposition. *J. Climate*, **8,** 352–360.

Palmer, T. N. and Sun, Z., 1985. A modelling and observational study of the relationship between sea surface temperature in the north-west Atlantic and the atmospheric general circulation. *Quart. J. Roy. Met. Soc.*, **111,** 947–975.

Peng, S. L., Mysak, A., Ritchie, H., Derome, J. and Dougas, B., 1995. The differences between early and midwinter responses to sea surface temperature anomaies in the northwest Atlantic. *J. Clim.*, **8,** 137–157.

Peng, S. and Whitaker, J., 1999. Mechanisms determining the atmospheric response to midlatitude SST anomalies. *J. Clim.*, **12,** 1393–1405.

Penland, C. and Sardeshmukh, P. D., 1995. The optimal growth of tropical sea surface temperature anomalies. *J. Clim.*, **8,** 1999–2023.

Penland, C., 1996. A stochastic model of IndoPacific sea surface temperature anomalies. *Physica D*, **98,** 534–558.

Pitcher, E. J., Blackmon, M. L., Bates, G. T. and Munoz, S., 1988. The effect of North Pacific sea surface temperature anomalies on the January climate of a general circulation model. *J. Atmos. Sci.*, **45,** 173–188.

Sardeshmukh, P. D., Compo, G. P. and Penland, C., 2000. Changes in probability associated with El Nino. *J. Clim.*, in press.

Winkler, C. R., Newman, M. and Sardeshmukh, P. D., 1999. An empirical low-frequency forecast model incorporating diabatic forcing. Proceedings of the Twenty-fourth annual Climate Diagnostics and Prediction Workshop, Tucson, AZ.